

Rapid, Efficient Ag-Au NPs Interdigitated Nano Biosensor Arrays for Water Quality Analysis

Report to the
Water Research Commission

by

**Mangaka Matoetoe, Caleb Duya, Bongiwe Silwana, Blessing Shekede &
Ziyanda Jabe**

Cape Peninsula University of Technology

WRC Report No. 2889/1/22

ISBN 978-0-6392-0247-1

July 2022



Obtainable from

Water Research Commission

Private Bag X03

Gezina

PRETORIA, 0031

orders@wrc.org.za or download from www.wrc.org.za

DISCLAIMER

This report has been reviewed by the Water Research Commission (WRC) and approved for publication. Approval does not signify that the contents necessarily reflect the views and policies of the WRC, nor does mention of trade names or commercial products constitute endorsement or recommendation for use.

EXECUTIVE SUMMARY

BACKGROUND

Escherichia coli (*E. coli*) and *Salmonella typhimurium* are commonly known bacterial contaminants in water and food. The presence of these bacteria in consumables remains a public health concern due to their high virulence and pathogenicity; causing common infectious gastrointestinal tract diseases in humans with symptoms such as diarrhoea. Presently, complex and lengthy microbial culture techniques (7 days) are used as common detection methods (Cabral, 2010). This has highly compromised the quality of human health. Hence, it is vital to develop a fast cost-effective method for the detection and quantification of these bacteria, thereby improving environmental monitoring, food quality and human health. Nanoparticles (NPs) have been shown as promising alternative chemicals for pathogen detection in biological samples (Nicolas-Chanoine, Bertrand and Madec, 2014; Allocati, Masuilli, Alexeyev and Di Ilio C, 2013). Thus, the project was aimed at combining the qualities of electro-analytical techniques and NPs in developing a sensor that is able to detect and quantify these bacteria in minutes. Electro-analytical techniques are preferred because they have unique advantages, such as high sensitivity, selectivity, low cost and are usually rapid.

AIMS AND OBJECTIVES

The following were aims and objectives of this project:

1. To synthesize silver-gold bimetallic nanoparticles (Ag-Au NPs) and binary quantum dots (QDs)
2. To characterize the chemical composition, morphology, optical and electrochemical properties of the bimetallic nanoparticles and binary QDs
3. To fabricate transducers and characterize them using the bimetallic NPs, binary QDs and fluorescence enhancer and antibodies
4. To optimize and validate the detection of *E. coli* and *Salmonella typhimurium* using the fabricated transducers
5. To fabricate, optimise and validate the interdigitated nanobiosensors, and application in real water samples

METHODS AND SUMMARY OF FINDINGS

The following nanomaterials were successfully chemically synthesised; monometallics (Ag NPs, Au NPs), Oxides (CuO NPs, ZnO NPs), Quantum dots (QDs) and bimetallic (Ag-Au NPs). The monometallics and bimetallics were synthesised using chemical reduction of the metal precursors with trisodium citrate while the oxides were synthesised via the heating of the precursor solution followed by slow addition of sodium hydroxide. The Glutathione capped AgInS ternary QDs were synthesised by slow addition of sodium hydroxide into a heated mixture of the Silver and Indium precursors followed by addition of the Sulphur precursors and the Glutathione. These QDs were coated with Zinc Sulphide by addition of the Zinc Sulphide precursors with continued heating. Verification and confirmation of the synthesised nanoparticles (NPs) was achieved through spectroscopy techniques such as UV-visible, Fourier Transform Infrared, X-ray and microscopic techniques such as Scanning Electron Microscopy (SEM) and Transmission Electron Microscopy (TEM).

The nanomaterials antibacterial and bacteria interaction was assessed through visual petri dish observation, optical or electrochemical measurement using *E. coli* and *Salmonella typhimurium*. Preliminary studies conducted showed that all the synthesised nanomaterials possessed antibacterial properties, with the monometallics and bimetallic being the most effective. Hence, they were subjected to further studies for bacterial interaction. Results from the bacteria interaction studies showed that the presence of *E. coli* resulted in a change in the absorbance and potential of the NPs optical and electrochemical measurements, respectively. These interaction studies were optimised for time, concentration of bacteria and concentration of nanomaterial. Generally, in all the NPs studied, the absorbance decreased with time as the reaction proceeded. The changes were also concentration dependent thus strongly suggesting possible bacteria detection using NPs. From the results obtained, it can be deduced that the NPs-bacteria interaction was mainly through the following:

- Electrostatic interaction with the nanomaterials since the bacteria are gram negative
- Abrasive damage of the cell walls thus forming nanomaterial-bacteria complex
- Plasmic membrane rupture exposing the bacteria content inside that changes the chemical environment of the solution
- Disruption of the biochemical process or triggering of electroactivity

The bacteria interaction studies were used in the fabrication of the film and non-film *E. coli* sensors for the bacteria. Differential pulse voltammetry (DPV), cyclic voltammetry (CV) and electrochemical impedance spectroscopy (EIS) were the main electroanalytical techniques used in this study. The choice of DPV, CV and EIS was based on their sensitivity, complexity, and portability respectively. These sensors had reasonable limit of detection (LOD), limit of quantification (LOQ) and linear ranges. They were further validated through recoveries of 90%. Preliminary studies of *Salmonella typhimurium* were also promising.

CONCLUSIONS AND RECOMMENDATIONS

The synthesis of monometallic (Ag NPs, Au NPs), Oxides (CuO NPs, ZnO NPs), Quantum dots (AgInS, AgInS/ZnS) and bimetallic (Ag-Au NPs) was successfully achieved. The synthesised materials were characterised spectroscopically and electrochemically for confirmation and establishment of both optical and electrochemical properties. The interaction of these nanoparticles with *E. coli* and *Salmonella typhimurium* were evaluated in order to establish the chemical reaction involved as well as the possibility of the utilisation of these interaction in detection. From the interaction studies the bimetallic NPs emerged as the best materials for possible application in fabrication of sensors of the bacteria due to their well-defined peaks of higher current and visible changes in signal observed as the bacteria concentration is varied. Sensors optimum conditions were assessed by fabrication and optimisation method. Electrochemical impedance spectroscopy, cyclic voltammetry, and differential pulse voltammetry were assessed for the signal monitoring of the sensors. EIS gave the best analytical parameters with an LOD of 10^1 and a linear range of 10^1 - 10^9 . Generally, the project execution efficiently managed with minimum challenges encountered due to COVID-19 and late signing of the agreement which resulted in inaccessibility to laboratory and problems in timely purchasing of required materials. The inaccessibility of relevant water sanitation offices prevented testing of the sensors in real water samples due to delayed acquisition of necessary sampling permits.

ACKNOWLEDGEMENTS

The project team wishes to thank the following people for their contributions to the project.

Name	Affiliation
Prof. Emmanuel Iwuoha	UWC SensorLab
Prof. Fanelwa Ajayi	UWC SensorLab
UCT SEM Unit	UCT
HRTEM Unit	UWC
Mr. Marvin Le Meyer	Research Officer, CPUT
Mrs. Zandi Mthembu	Laboratory Technician, CPUT

CONTENTS

EXECUTIVE SUMMARY	iii
ACKNOWLEDGEMENTS	v
CONTENTS	vi
LIST OF FIGURES	viii
LIST OF TABLES	viii
ACRONYMS & ABBREVIATIONS	ix
CHAPTER 1: BACKGROUND	1
1.1 INTRODUCTION	1
1.2 PROJECT AIMS	3
1.3 SCOPE AND LIMITATIONS	3
CHAPTER 2: SYNTHESIS AND CHARACTERISATION OF NANOMATERIALS	4
2.1 INTRODUCTION	4
2.2 METHODS	4
2.2.1 Synthesis of nanoparticles and characterisation	4
2.2.2 Synthesis of AgInS QDs and AgInS/ZnS QDs.....	5
2.2.3 Characterisation of synthesised materials	5
2.3 RESULTS AND DISCUSSIONS	6
2.3.1 Monometallic and oxides	6
2.3.2 Preliminary assessment of antibacterial properties of the synthesised nanomaterials	7
2.3.3 Quantum dots.....	7
2.3.4 Bimetallic spectroscopic characterisation of synthesised nanoparticles	8
2.3.5 Electrochemical characterisation	10
2.4 SUMMARY	11
CHAPTER 3: SENSORS FABRICATION, OPTIMISATION AND VALIDATION	12
3.1 INTRODUCTION	12
3.2 MATERIALS AND METHODS	13
3.2.1 Cell cultures	13
3.2.2 Optimization of parameters for bacteria-nanoparticles interaction studies.....	14
3.2.3 Sensors analytical parameters.....	14
3.3 RESULTS AND DISCUSSION	14
3.3.1 Interaction of nanoparticles with bacteria	14
3.3.2 Sensor fabrication for detection of <i>E. coli</i>	16
3.3.3 Sensor Optimisation.....	17
3.3.4 Calibration and analytical parameters	18
3.3.5 Mechanism for bacteria redox activity	21
3.4 SUMMARY	22

CHAPTER 4: CONCLUSION AND RECOMMENDATIONS	23
4.1 CONCLUSIONS.....	23
4.2 RECOMMENDATIONS.....	23
REFERENCES	24

LIST OF FIGURES

Figure 1-1:	Pathogenic bacteria studied (a) <i>E. coli</i> (Kock, 2019), (b) <i>Salmonella typhimurium</i> and (c) Symptoms of Salmonellosis	1
Figure 2-1:	Monometallic and oxides characterisation; TEM images and size distribution of (A) Ag NPs (B) CuO NPs, (C) ZnO NPs	6
Figure 2-2:	The XRD spectra of the Monometallic NPs and oxides NPs	6
Figure 2-3:	<i>In vitro</i> effect of different concentrations of nanomaterials on <i>E. coli</i> after 24 hours (a)Ag NPs (b) CuO NPs and (c) ZnO NPs	7
Figure 2-4:	Spectroscopic characterisation of quantum dots; AgInS core QDs and AgInS/ZnS core/shell; (a and b) SEM images, (c) absorption(c), (d) PL and (e) FTIR	8
Figure 2-5:	Spectroscopic characterisation of the Ag-Au (1:2) bimetallic NPs ((a) UV-visible, (b) FT-IR and (c) XRD) (I) and SEM images of (a) Ag-Au NPs, (b) Au NPs and (c) Ag NPs (II).....	9
Figure 2-6:	The voltammogram of the chemical modified glassy carbon electrodes (GCE) with.....	10
Figure 3-1:	UV-visible absorption spectra interactions of various concentration of <i>E. coli</i> and <i>Salmonella typhimurium</i> bacteria with nanoparticles and (a) Ag NPs, (b) Au NPs and (c) Ag-Au (2:1) NPs	15
Figure 3-2:	Cyclic voltammetry detection of the <i>E. coli</i> and <i>Salmonella typhimurium</i> (ST) bacteria using a) Ag NPs, b) Au NPs and c) Ag-Au NPs in 0.1 M PBS. PH 7.4.....	16
Figure 3-3:	The differential pulse voltammograms (DPV) for detection of <i>E. coli</i> (a) and	17
Figure 3-4:	Sensor fabrication optimisation and experimental optimisation for DPV sensors	18
Figure 3-5 :	Typical (a) DPV voltammograms and (b) EIS Nyquist plot responses of the sensors to varying concentrations of <i>E. coli</i> as well as the corresponding calibration plot of ΔR_{ct}^{-1} versus log of <i>E. coli</i> concentrations.	19

LIST OF TABLES

Table 3-1:	Comparison of reported nano-impact electrochemical techniques for <i>E. coli</i> detection with the developed methods	22
------------	---	----

ACRONYMS & ABBREVIATIONS

CV	Cyclic voltammetry
DPV	Differential pulse voltammetry
<i>E. coli</i>	Escherichia coli
EIS	Electrochemical impedance spectroscopy
FTIR	Fourier transform Infrared
NPs	Nanoparticles
QDs	Quantum dots
SEM	Scanning electron microscopy
ST	Salmonella typhimurium
TEM	Transmission electron microscope
UV Visible	Ultraviolet visible spectroscopy

CHAPTER 1: BACKGROUND

1.1 INTRODUCTION

Microorganisms are present almost everywhere and they are utilised in industrial, clinical and environment (Ferens and Hovde, 2011). Reports on outbreaks of infectious diseases and consumables poisoning is prevalent. Hence, contamination of food, drugs, water, cosmetic products with microorganisms or their derivatives is a concern for industries productivity (Heredia and García; 2018). Hence monitoring is necessary to ensure quality water for manufacturing and consumption to minimise product contamination. An effective monitoring necessitates a timely, sensitive, cost-effective technique that can be run ideally online or on site to detect dangers and compromised materials. The commonest monitoring techniques are for detection of *E. coli* and *Salmonella typhimurium* as they are regarded as indicators of presence of microorganisms and are usually the cause of the outbreaks (Todd, Greig , Bartleson and Michaels, 2008; Ansari et al., 2013). The structure of the bacteria and symptoms associated with the common outbreaks of Salmonellosis are depicted in Figure 1-1 (a, b and c).

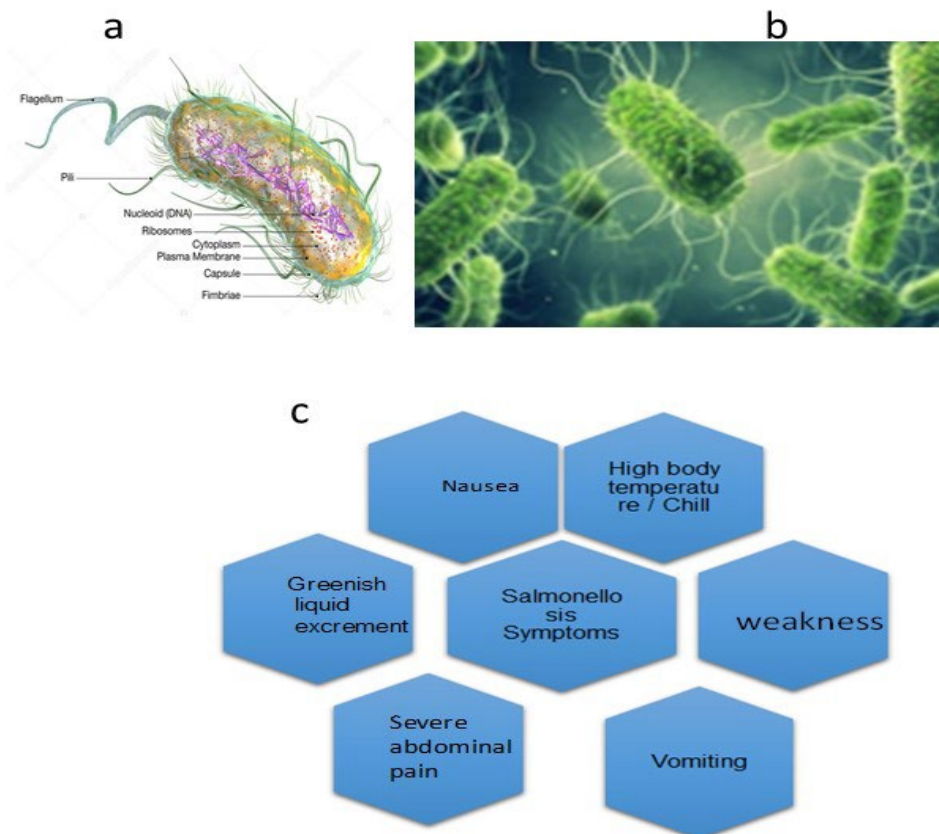


Figure 1-1: Pathogenic bacteria studied (a) *E. coli* (Kock, 2019), (b) *Salmonella typhimurium* and (c) Symptoms of Salmonellosis

The two bacteria are Gram-negative bacteria therefore belonging to a large group of family known as *Enterobacteriaceae* (Nicolas-Chanoine, Bertrand and Madec, 2014). They both typically live in animals and human intestines, finding their way into the water sources through faeces ((Ferens and Hovde, 2011). Thus infection is most frequently through contaminated water causing salmonellosis and shiga-toxin from *Salmonella typhimurium* and *E. coli* respectively (Heredia and García, 2018). It is reported that *E. coli* cells of approximately 10 to 100 in human faeces can induce shiga-toxin type 2 infections in humans (Todd, Greig, Bartleson and Michaels, 2008). Symptoms of these illness are similar and appear as depicted in Figure 1-1c.

These illnesses have globally led to about 1.6 million fatalities especially among children under the age of five years.⁷ Infectious diarrheal disease transmitted by *E. coli* and *Salmonella typhimurium* has also registered an annual global death of about 485,000 due to poor water quality, sanitation and hygiene (WHO, 2017). Presence of *E. coli* is always used as an indicator of faecal contamination and heightened risk of availability of *Salmonella typhimurium* (Li et al., 2012). Water is declared of high risk for consumption when *E. coli* cells are between 100 and 1000 colony forming unit per millilitre (CFU/mL) (Stromberg et al., 2017). There is no confirmed cure for *E. coli* and *Salmonella typhimurium* infections and the use of antibiotics increases the risk of contracting haemolytic uremic syndrome and haemorrhagic colitis diseases (Freedman, 2018). Other reports showed that the use of antibiotics slow down digestive system thereby decreasing the body's ability to eliminate toxins efficiently (Schiller, Pardi and Sellin, 2017) The prevalence of *E. coli* and *Salmonella typhimurium* infections their serotypes multiplicity in water sources necessitates the use of a rapid sensitive and selective detections. An issue that is currently a challenging task for researchers (Plaza et al., 2018). Hence, culture-based techniques have continued being the gold standard method for most bacterial detections and identification in the recent past (Hilton et al., 2016). However, the major drawback is that they are time-consuming as they require about 7-8 days to obtain results (Zhang et al., 2019). In addition, skilled labour and sophisticated laboratory set-ups are required hence limiting their applications in some locations lacking such facilities (Smith et al., 2019).

The introduction of nanotechnology has opened the research in alternative detection methods where several platforms have been developed for *E. coli* and *Salmonella typhimurium* detections with high sensitivity and specificity. These techniques include immuno-based sensing, molecular techniques, mass spectrometry (MS), loop-mediated isothermal amplification (LAMP) and next generation sequencing (Walper et al., 2018). Although these assays have shown higher sensitivity and specificity, they still require longer analysis time, use of sophisticated laboratory equipment, highly skilled personnel and laborious sample preparation stages which limit their widespread application (Niessen, Luo, Denschlag and Vogel, 2013). Therefore, there is still an enormous unmet need for faster, easy to use, cost-effective and highly sensitive on-site detection techniques. Some of the techniques have recently been developed to improve sensitivity and selectivity including electrochemical biosensors, surface-enhanced raman scattering (SERS), fluorescent assays, optical sensors, localized surface plasmon resonance (LSPR) and nano-biosensors (Umesha and Manukumar, 2018).⁹

In addition, detection techniques of *E. coli* and *Salmonella typhimurium* using electrochemical biosensing have been reported (Li et al., 2012). These involve detections of sample analytes by measuring the changes in electrical properties of the electrode surface (Wang, Ye and Ying, 2012). These biosensors have significantly attracted attention of most researchers due to their simplicity, faster analysis response, comparable sensitivity,

ability to operate in turbid solutions, higher possibility of miniaturization and amenability towards integration into one simple, automated and low-cost devices using new technology such as nanomaterials (Arora, Ahamed, Sucheta and Siddiui, 2018). However, their use in the detection of complex samples has brought many challenges because they can only detect single species of analytes on a single interface and require larger amount of samples and reagents hence unable to meet the current demand of low-cost-multiplexed detections (Ojea-Jiménez, Bastús and Puntés, 2011). Therefore, direct use of these devices in the detection of bacteria in water matrices is quite challenging without proper and appropriate sample collections and preparations. Moreover, the complexity of water matrices can vary based on content, formality and viscosity which can also greatly affect sensitivity and selectivity of the biosensor ((Freedman, 2018). With the emergence of sophisticated biotechnology and nanotechnology, research in the development of these biosensors for specific detections of *E. coli* and *Salmonella typhimurium* in complex sample matrices have been focused on the improvement of novel bio-receptors, better electrode designs and use of novel nanomaterials for effective electron transduction (Plaza et al., 2018). Novel nanomaterials with enhanced biocompatibility and surface area to volume ratio can be used as nanocarriers to increase the number of probes immobilized onto the electrodes of these biosensors thereby enhancing their sensitivity, selectivity and multiplex detection ability (Umesha and Manukumar, 2018).

1.2 PROJECT AIMS

The following are aims and objectives of this project:

1. To synthesize silver-gold bimetallic nanoparticles (Ag-Au NPs) and binary quantum dots (QDs)
2. To characterize the chemical composition, morphology, optical and electrochemical properties of the bimetallic nanoparticles and binary QDs
3. To fabricate transducers and characterize them using the bimetallic NPs, binary QDs and fluorescence enhancer and antibodies
4. To optimize and validate the detection of *E. coli* and *Salmonella typhimurium* using the fabricated transducers
5. To fabricate, optimise and validate the interdigitated nanobiosensors, and application in real water samples

1.3 SCOPE AND LIMITATIONS

The project focused on the syntheses of monometallic NPs, bimetallic NPs and quantum dots. The synthesised material's properties and interaction with the pathogenic bacteria studied were assessed. Based on the outcome of the properties and the interaction studies, a suitable material was assessed for sensors fabrication. The fabrication of the sensor using three electrochemical techniques were optimised, evaluated, and validated. However, the synthesis optimisation was not done. In-depths analysis of the nanoparticles which were not used for sensor fabrication was not pursued. Real sample surface water analysis on site and off site were also not carried out. Hence, the study was confined only to method development studies with minimum validation experiments. Comparison of the effectiveness of the sensors developed to approved analytical methods was not evaluated.

CHAPTER 2: SYNTHESIS AND CHARACTERISATION OF NANOMATERIALS

2.1 INTRODUCTION

Nanomaterials have a vital role in materials science, chemistry, physics and, medicine, already finding applications in several fields, including therapeutic, diagnostic and sensors (Hilton et al., 2016). According to research, the preparation of nanoparticles depends on many experimental conditions, including the choice of reducing agent. Understanding the reasons for the aggregation, shape, surface, and change of size of the nanoparticles after integration into a target application is critical for optimising performance. Among metallic nanoparticles, silver nanoparticles (Ag NPs) are the most studied nanomaterials due to versatility in synthesis, easy processing, and fast kinetic reaction rate, high thermal and chemical stability. In addition, Ag NPs often have general dispersibility and wide size distribution, which may inevitably generate imprecise results (Walper et al., 2018).

Countless procedures have been used for the preparation of nanomaterials. However, wet chemical reduction process is one of the simplest and advantageous methods with a better yield compared to physical procedures. Wet chemical methods timeously use three main components, which are metal precursors, reducing agents, and stabilising/capping agents. In most of the synthesis methods, reducing agents are used in excess with regards to stoichiometric quantities. This makes complications to the process. It is important to mention that the current tendency is to find reaction conditions where the reducing agent is also in charge of directing the structure and being a stabiliser of the final product. The synthesised materials were cleaned thoroughly three times using pure distilled water centrifugation.

To ascertain purity and confirm the formation of the desired material, characterisation of the material was carried out using spectroscopy and electrochemistry. In addition to the materials properties, their potential for electrochemical transduction was determined.

2.2 METHODS

2.2.1 Synthesis of nanoparticles and characterisation

The monometallic nanoparticles were synthesised using the precursors AgNO_3 and HAuCl_4 for Ag NPs and Au NPs respectively. The oxides CuO NPs and ZnO NPs were synthesised using Cu and Zn nitrates salts. The precursor solutions, chemical reduction was carried out using tri-sodium citrate (TSC) for the monometallic at a controlled temperature similar to what is outlined below for bimetallic. The oxides formation was achieved through the slow addition of sodium hydroxide into heated precursors solution. While the bimetallic Ag-Au NPs of different molar ratios (1:1, 1:2, 2:1) respectively and concentrations of (5, 10, 15 mM) of Ag-Au bimetallic nanoparticles were synthesised via co-reduction of Ag and Au precursors using TSC as both reducing and capping agent. To a 100 mL Erlenmeyer flask, 20 mL of metal precursors AgNO_3 (5×10^{-3} M) together with

40 mL of HAuCl_4 (2.5×10^{-3} M) was heated to boiling at a constant temperature of 240°C under vigorous stirring followed by addition of 2 mL of 2% TSC. The reaction mixture was then heated for another hour under vigorous stirring and the yellow coloured solution appeared indicated the formation of bimetallic Ag-Au NPs. In repeated synthesis steps, the volume of the mixture was adjusted accordingly in order to prepare Ag-Au NPs with molar ratios of 1:1, 1:2 and 2:1. The solution was then allowed to cool naturally under vigorous stirring to minimise agglomeration of the nanoparticles. The nanoparticles were then centrifuged at 10,000 rpm for 15 minutes to remove impurities and cleaned with distilled water three times.

2.2.2 Synthesis of AgInS QDs and AgInS/ZnS QDs

Glutathione capped AgInS core quantum dots (QDs) were synthesised as follows: AgNO_3 (0.0107 g, 0.063 mmol), InCl_3 (0.055 g, 0.25 mmol), $\text{Na}_3\text{C}_6\text{H}_5\text{O}_7$ (0.294 g, 1.00 mmol), GSH (0.045 g, 0.145 mmol) were added to 100 mL of deionised water under magnetic stirring in a 250-mL three-neck flask. The pH was adjusted to 7.5 by adding of small amounts of NaOH (1.0 M). Na_2S (0.0975 g/10 mL, 1.25 mmol) was then added under vigorous magnetic stirring and the resulting solution was refluxed at 95°C for 45 min to form AgInS core QDs. After this period, $\text{Zn}(\text{O}_2\text{CCH}_3)_2(\text{H}_2\text{O})_2$ (0.044 g/10 mL, 0.200 mmol) and $\text{CH}_4\text{N}_2\text{S}$ (0.015 g/10 mL, 0.200 mmol) were added to the reaction mixture, which was then refluxed for 1 hr 20 min at 95°C to form AgInS/ZnS core/shell QDs. The experimental conditions for the synthesis of QDs were optimised by assessing the effect of reaction time, Ag/In ratio and number of ZnS coatings required for the preparation of luminescent and water-soluble AgInS/ZnS core/shell QDs. For the precipitation of the obtained QDs, 200 mL of ethanol ($\text{C}_2\text{H}_5\text{OH}$) was added, and the mixture was centrifuged. The precipitate was collected and re-dispersed in water, and the procedure was repeated two times. The obtained QDs samples were stored in amber glass vials at room temperature.

2.2.3 Characterisation of synthesised materials

The optical properties of nanoparticles were investigated using double beam UV-visible 1800-Shimadzu spectrophotometer, Advanced African Technology (Scientific division) serial number 127471. FTIR investigations were done using a PerkinElmer Spectrum Two apparatus in the wavelength range of 600 to 3000 cm^{-1} . The two powdered samples were placed on the diamond eye and pressed using the pressure applicator. The Silver gelatinous fluid was dropped using a pipette dropper and analysed. The size distribution and morphology were analysed using a SEM. The SEM images were then analysed by image J, java-based image processing program. Electrochemical measurements were run using a typical conventional one-compartment three electrode system connected to potentiostat Autolab PGSTAT 101 (Metrohm, SA) operating in software NOVA 2.1. Three electrode cell set-ups consisted of GCE, a platinum wire and Ag/AgCl electrode. The GCE was polished with 0.05, 0.3 and $1\ \mu\text{m}$ alumina powder to remove any residue deposits on the surface. As part of daily polishing routine, the GCE was sonicated in water and ethanol for 5 min in between polishing steps. All experiments were run using 0.1 M HCl solution over a potential range -0.5 to $+0.5$ V.

2.3 RESULTS AND DISCUSSIONS

2.3.1 Monometallic and oxides

The spectrophotometric and electrochemical characterisation of the synthesised monometallic and oxides confirmed that the desired nanomaterials were synthesised. The spectra and images (Figure 2-1) obtained corresponded with previous related studies (Walper et al., 2018). An average particle size of 22.3, 38 and 21 nm for Ag NPs, CuO NPs and ZnO NPs were calculated respectively as shown in Figure 1-1. The voltammogram peak potentials confirmed synthesis of Ag NPs, CuO NPs and ZnO NPs respectively as seen in Figure 2-2.

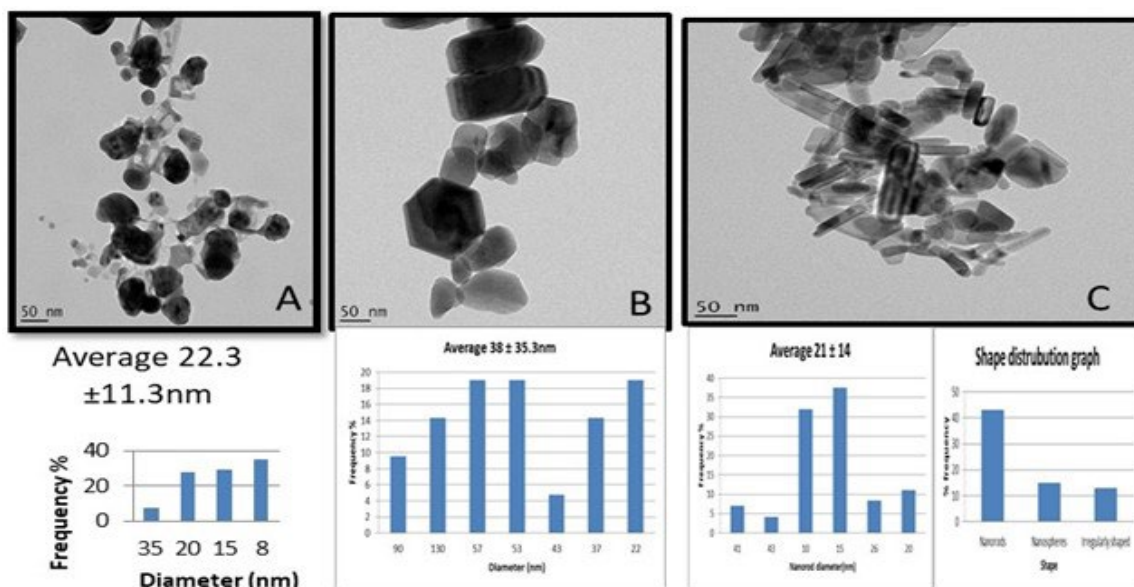


Figure 2-1: Monometallic and oxides characterisation; TEM images and size distribution of (A) Ag NPs (B) CuO NPs, (C) ZnO NPs

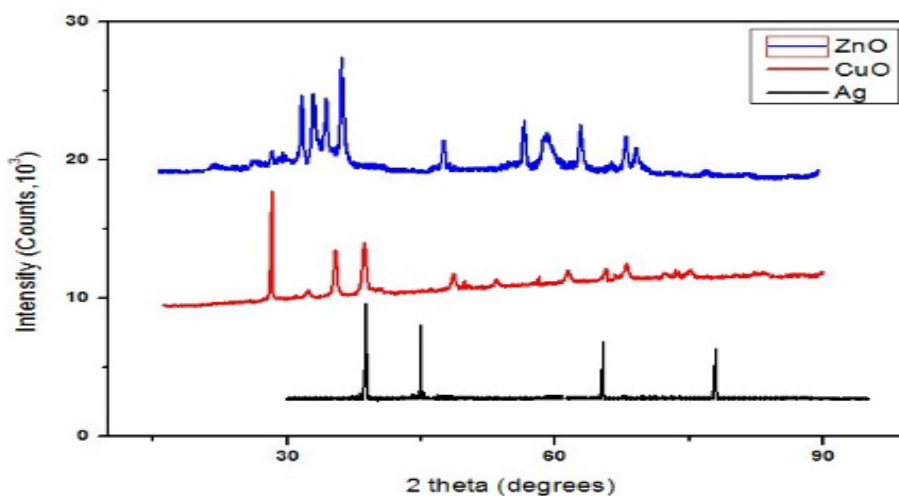


Figure 2-2: The XRD spectra of the Monometallic NPs and oxides NPs

2.3.2 Preliminary assessment of antibacterial properties of the synthesised nanomaterials

The antibacterial properties of the synthesised nanomaterials were assessed with *E. coli* using plate culture as depicted in Figure 2-4. All the synthesised materials showed some degree of antibacterial activity. A varying degree of bacteria varied response was observed from the various materials. However, Ag NPs had a better response compared to the oxides. Hence Ag NPs was chosen for further studies and the results presented in Chapter 3.

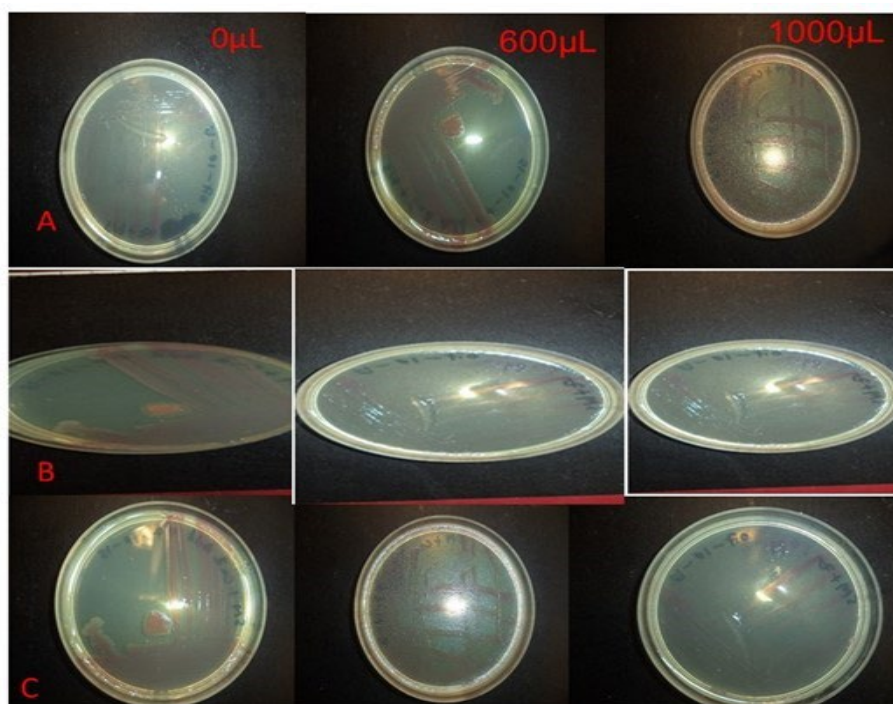


Figure 2-3: *In vitro* effect of different concentrations of nanomaterials on *E. coli* after 24 hours (a)Ag NPs (b) CuO NPs and (c) ZnO NPs

2.3.3 Quantum dots

Ternary I–III–VI quantum dots (QDs) have proved to be promising alternatives to the traditional binary Cd-QDs due to their inherently lower toxicities, greener synthetic methods, and tuneable optoelectronic properties. Their application in the development of biosensors, electroluminescent devices, and a range of other electrochemical applications has resulted in the I–III–VI QDs receiving widespread attention in various fields. Water-soluble glutathione capped AgInS core QDs and AgInS/ZnS core/shell QDs were synthesized using an eco-friendly hydrothermal method. The optical data and SEM image of the synthesised QDs is depicted in Figure 2-5.

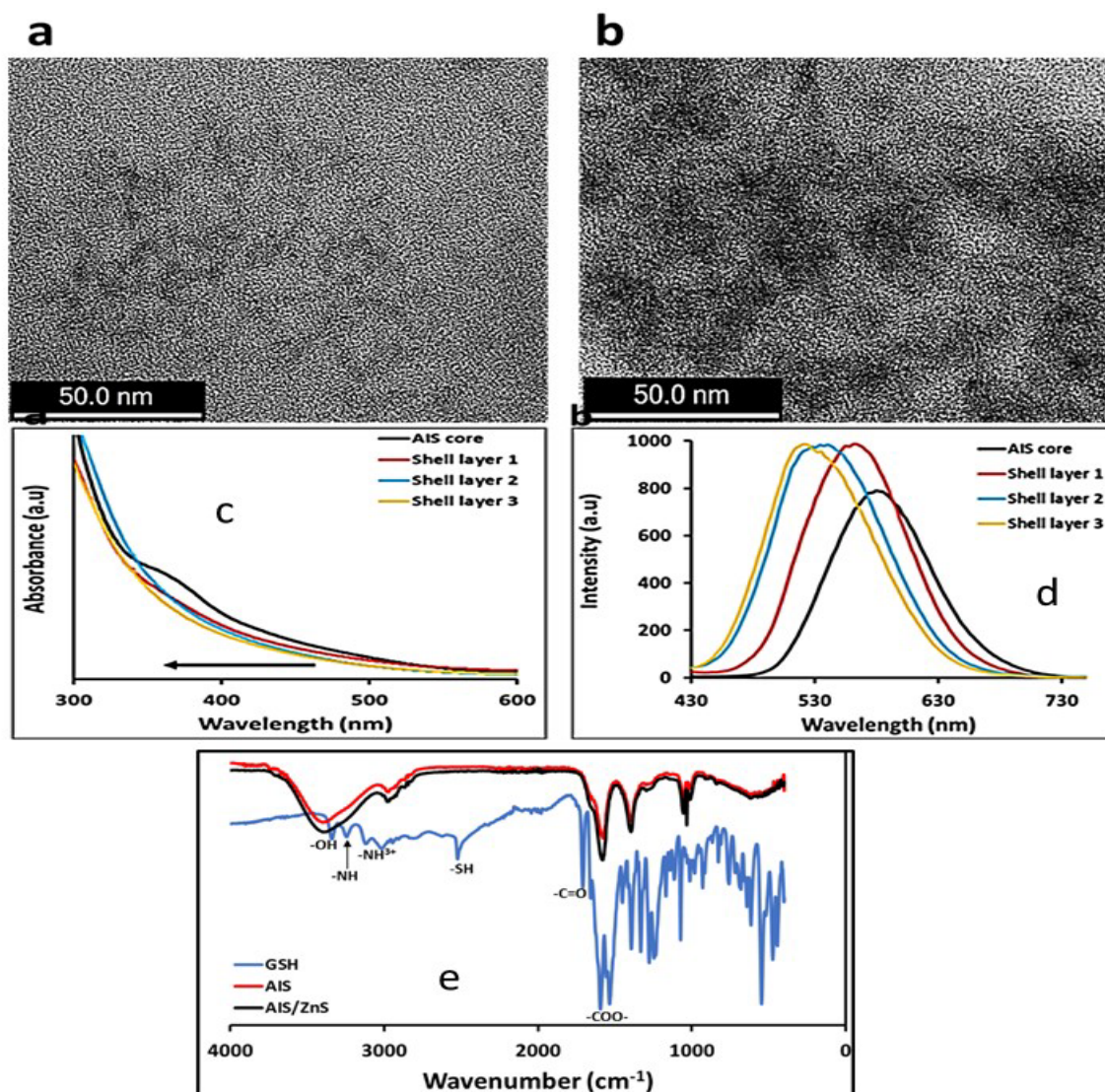


Figure 2-4: Spectroscopic characterisation of quantum dots; AgInS core QDs and AgInS/ZnS core/shell; (a and b) SEM images, (c) absorption(c), (d) PL and (e) FTIR

The SEM image Figure 2-5a and b showed similar morphology for both core and core/shell QDs with acceptable sizes for QDs. Physical and chemical properties suggest that the NPs and QDs are suitable for the development of biosensors. However, preliminary results of the bacterial interaction were not consistent. This can be because the reactions were too fast for an accurate monitoring. Parameters optimisation is required in order to have an understanding of the interaction. Hence, this material was not used for further studied since a number of factors still require studies. The optical properties shown by Figure 2-5c and d for photoluminescence and absorption showed that the QDs are depended on the shell layer. An increase in shell layer resulted in an increase in optical properties for both techniques. The synthesized AgInS core QDs and AgInS/ZnS core-shell QDs exhibited chemical and physical properties which depend on synthesis parameters.

2.3.4 Bimetallic spectroscopic characterisation of synthesised nanoparticles

In order to improve on the bacterial activity of the bimetallic NPs of Ag and Au was synthesised. The synthesised bimetallic's UV-visible spectra Figure 2-6(a) showed the presence of two distinct and intense

plasmon bands centred at 413 and 525 nm confirming the synthesis of Ag-Au (1:2) NPs. The spectrum depicts a low intensity, narrower LSPR of Au NPs. Thus, suggesting that the synthesized bimetallic NPs comprised of smaller-sized Au NPs compared to Ag NPs. While the FTIR spectra confirmed citrate-capped Ag-Au (1:2) NPs. The distinct sharp and broad peaks at 1745 and 3320 cm^{-1} signified the presence of -C=O and -O-H bond stretches, respectively. This was due to the formation of oxidative by-products of TSC including dicarboxyacetone, itaconic acid, acetoacetate and carbon (IV) oxide.²⁰ The broadness of the absorption band at 3320 cm^{-1} was attributed to hydrogen bonding between water molecules as similarly reported elsewhere.²³ The characteristic absorption band at 1068 cm^{-1} indicated -C-O-C- bond stretching vibrations from the citrate ion capping the NPs thus showed the presence of TSC.

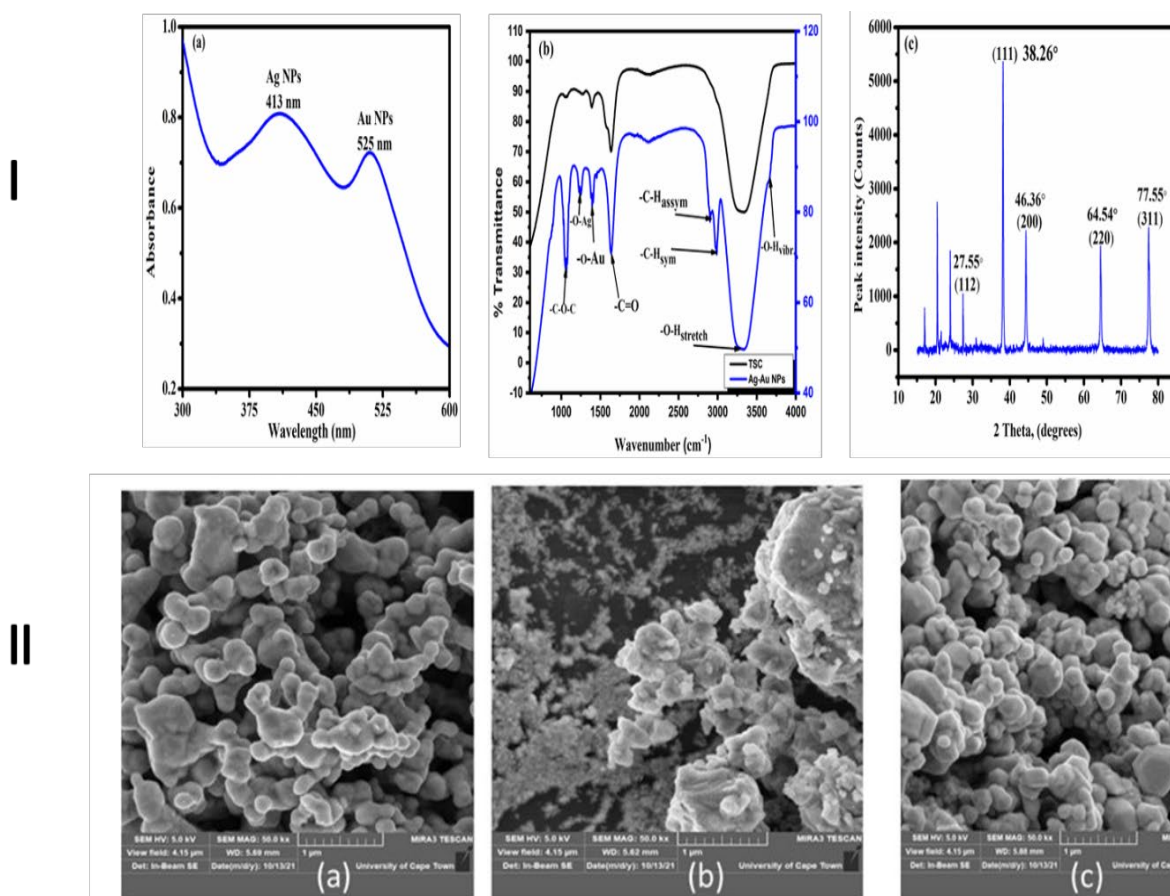


Figure 2-5: Spectroscopic characterisation of the Ag-Au (1:2) bimetallic NPs ((a) UV-visible, (b) FT-IR and (c) XRD (I) and SEM images of (a) Ag-Au NPs, (b) Au NPs and (c) Ag NPs (II).

The XRD pattern in Figure 2-6(I)c showed four main diffraction peaks at $2\theta = 38.26^\circ$, 46.36° , 64.54° and 77.55° corresponding to (111), (200), (220) and (311), crystallographic planes of face-centred cubic Ag-Au NPs, respectively (JCPDS card no. 04-0785). This can be attributed to the presence of bulk Ag and Au with closely similar lattice parameters (Ag-0.409, Au-0.408 nm). The lattice plane of (111) was the most intense and this can be ascribed to its higher free energy and faster growth rate.

The SEM images are depicted in Figure 2-6 (II)a to c. The monometallics and bimetallic has a cauliflower morphology. Both Ag NPs (Fig. 2-6(II)a) and Au NPs (Fig. 2-6(II)b) depicted slightly agglomerated distinct spherical structures. However, unique agglomeration patterns and nanosized further confirmed the synthesis

of nanomaterials. The SEM image indicated that the obtained bimetallic NPs were of high dispersity with larger-sized particles. Similar morphology has been reported.

2.3.5 Electrochemical characterisation

Electrochemical characterisation was made of synthesised materials films as described in the method section. The chemical modified electrodes were studied using cyclic voltammetry. The voltammogram of the bare GCE (Figure 2-7 GCE Ag NPs showed no peaks indicating that it is non-electroactive. However, the modified GCE (GCE/Ag NPs, GCE/Au NPs and Ag-Au NPs) had characteristic redox peak at the appropriate potential indicative of the metals. Figure 2-7; GCE/Ag NPs had a sharp oxidation (a) and reduction (a') peaks at +0.54 V and +0.49 V, respectively corresponding to the Ag/Ag⁺ couple. These are attributed to the enhanced electroactivity of the modified GCE due to the presence of Ag NPs thin film. The sharp oxidation and reduction peaks can be ascribed to faster electron transfer rates due to the electroactive nature of Ag NPs on the GCE surfaces as similarly described elsewhere.²² The voltammogram for GCE/Au NPs showed oxidation (b) and reduction (b') peaks typical of gold oxide monolayer formation and reduction at +1.51 V and +0.53 V, respectively (Figure 2-7 GCE/Au NPs). This is in close agreement with a study reported in the literature showing the formation of a cathodic peak of Au between a potential range of +0.2 and 0.6 V due to the reduction of gold oxide formed during anodic cycle. The authors attributed this to the wider positive potential window used in their study (Chen et al., 2021).

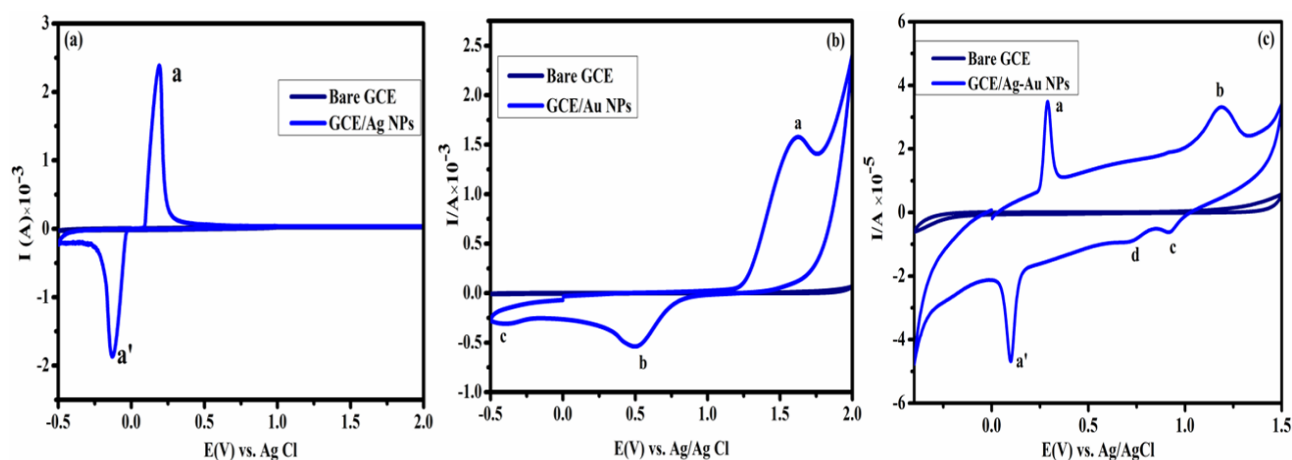
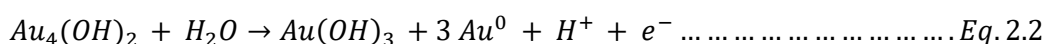


Figure 2-6: The voltammogram of the chemical modified glassy carbon electrodes (GCE) with Ag NPs.

The CV responses of GCE/Ag-Au NPs (2:1) showed two well defined anodic Au NPs and Ag NPs peaks (+0.47 V, +1.50 V represented as **a** and **b**, respectively) and three cathodic peaks (+0.35 V, +0.93 V and +1.16 V shown as **a'**, **c** and **b'**, respectively). Thus, confirming presences of both Ag and Au in the bimetallic arrangement. Similar shaped peaks have been reported¹⁹. Possible chemical reactions responsible for the observed peaks can be explained by Eq. 2.1 to Eq. 2.5. The shapes of the peaks in the voltammogram indicates that during the analysis, the redox reaction of Ag NPs was relatively faster than Au NPs with enhanced cathodic

and anodic peak currents. This is attributed to faster electron transfer rates as depicted by the sharper anodic and cathodic peaks of Ag NPs with higher peak currents as compared to those of Au NPs. It can also be due to the ratio of the metals in the bimetallic with Ag being more concentrated. These electrochemical properties confirmed the major electrical contribution by Ag in the GCE/Ag-Au (2:1) NPs as similarly shown in the molar ratio of Ag: Au (2:1). The anodic peak at +1.50 V can be related to the oxidation of Au⁰ to gold trihydroxide (Au(OH)₃) which was in turn reduced to Au²⁺ at +1.16 V. Oxidation of Au at +1.17 V to Au(OH)₃ has also been reported in the literature.²⁸ The appearance of a cathodic peak at around + 1.15 V for Au reduction has also been reported in the literature.²³ Possible reaction taking place at Au are summarised below;



2.4 SUMMARY

Synthesis of several metal nanoparticles and quantum dots were successful as confirmed by the FTIR, UV-visible and TEM Studies. The data obtained from these techniques is comparable to literature and indicates that the materials synthesised were pure. All the synthesised materials particles sizes ranged from 10 nm to 40 nm which is within the nanoscale thus confirming syntheses of nanoparticles. They are all optically and electrochemically active. All metal and metal oxides NPs were found to be bactericidal with Ag NPs being the best and the oxides the least. Quantum dots synthesis was also confirmed through particle size, optical activity and FTIR. However, bacterial interaction assessments was not effectively assessed due to fast reaction times as well as low yields. Further studies are required to improve production yield of QDS and to optimise the interaction studies. Based on these results monometallic and bimetallic NPs were further studied for nanoparticle bacteria interactions and fabrication of the sensors.

CHAPTER 3: SENSORS FABRICATION, OPTIMISATION AND VALIDATION

3.1 INTRODUCTION

Research on the development and application of commercially available bacteria detection methods have been ongoing. The methods are categorized based on principle applied in their analysis. The groups are conventional culture methods, immunology-based assays, nucleic acid-based assays, miniaturized biochemical assays, and biosensors. Conventional culture methods predominate the food testing laboratories. The most popular methods used to determine these microbes involve microbial culture and plate counting agar (PCA) using selective medium. These methods are accurate and consistent however, they require long cultivation periods which are time consuming in the laboratory. Some of the common methods used for detection of *E. coli* includes the following techniques; Gunda , Dasgupta and Mitra, 2017 used a litmus paper (Dip test) to detect *E. coli* in water samples by performing enzymatic reactions directly on porous paper substrate. Possible interfering bacteria and chemical contaminants for Dip test device have been assessed and found to have no impact on its results. Hence, it can become a potential solution for screening water samples for *E. coli* contamination.

One of the major problems in developing a rapid test for pathogens is the massive and complex machine used, including extensive upgrading procedures. Although faster technique for detecting *E. coli* in water such as polymerase chain reaction and enzyme-linked immunosorbent assay have been developed, it still required transporting the samples from water resources to the laboratory, high-cost, complicated equipment usage, complex procedures, it requires a skilled specialist to cope with the complexity which limit their wide spread practice in water quality detection (Arora, Ahamed, Sucheta and Siddiui, 2019). Nanomaterials sensors are an attractive proposal for analytic and bacteria detection in this research area.

Recent discovery of nanomaterials has resulted in an increased report on their usage in bacterial control showing better signs of effectiveness than other convectional anti-bacterial methods (Muhammad et al., 2017). The nanoparticles used as bactericidal or antibiotic agents are normally biologically active and either inorganic or organic in nature. Bulk metallic elements such as Copper, Zinc, Titanium and Silver have notable antibiotic properties as a result they were utilised in the past for the treatment of mild infections and as bacterial prophylaxis agents both internally as well as in the epidermal cavity (Chen et al., 2021). It is then expected that as these naturally antibacterial metals approach their nano size range, they should have an increased bactericidal effect since the surface area to volume ratio increase as size decreases. Other metallic elements like Iron are not bactericidal in their bulk form but have been reported to exhibit bactericidal effects as their size goes below 80 nm and this makes them potential bactericidal agents (Guanye et al., 2018). This takes into account the hypothesis that bactericidal capability of the nanoparticles is dependent on the surface area to volume ratio of the nanoparticles and their morphology.

Therefore, these nano-scale attributes of metallic nanoparticles pose great potential for their use as modern

day antibiotics. Studies show that different types of metallic nanoparticles behave differently towards the vast species of bacteria available (Lee et al., 2016). Therefore, bactericidal efficacy of the nanoparticles must be evaluated in order to appropriately pair some metallic nanoparticles with the bacteria they can effectively combat. Metallic metals that have been investigated vastly as potential antibiotics are Silver, Zinc, Copper, Gold, Aluminium, Titanium and Iron (Sepunaru et al., 2015). Besides the efficacy factor, the issues of relative toxicity and economics come into play. It is more favourable for the nanoparticles that are economic in terms of synthesis and production to be used as an antibiotic in order to prevent the economic cons outweighing the advantages of the nanoparticles as bactericidal agents. Metallic nanoparticles usage as bactericidal agents are mainly due to their economic advantage as a result of their economically established method of synthesis. Nanoparticles have shown remarkable bactericidal and bacteriostatic effects in bacterium that has been previously resistant to conventional antibiotics (Ronspees and Thorgaard, 2018).

The mechanism against bacteria for the various nanoparticles differs (Figure 3-7) from one material to another but their bactericidal strength lies in their large surface area to volume ratio which makes the particles very reactive and small enough to penetrate through cyto-pores of bacterial cell walls. The morphology of the particular nanoparticles has shown to affect the effectiveness and efficacy of the nanoparticles in the elimination of bacteria (Couto , Chen , Kuss and Compton, 2018). The bactericidal effects of nanoparticles have also been shown to be influenced by the type, dimensions and shape of the nanoparticles (Chen et al., 2021). The methods of administration of nanoparticles as complementary bactericides are broad due to their relative solubility and ability to be incorporated in composites and hybrids with other material. As bactericidal agents, nanoparticles have been incorporated in creams, ointments and epidermal fluids (Lee et al., 2016). Metal oxide nanoparticles have been used for the modification of textiles functionalizing the textiles to be antimicrobial clot.

3.2 MATERIALS AND METHODS

3.2.1 Cell cultures

Escherichia coli ATCC 25922 bacteria were donated by Microbiology Laboratory, Cape Peninsula University of Technology, Cape Town, South Africa and stored as frozen stocks at -10°C before cultivation. The bacteria were then cultivated using Brain Heart infusion (BHI) broth containing 17.5 g/L porcine, 10.0 g/L tryptose, 2.0 g/L glucose, 5.0 g/L NaCl and 2.5 g/L Na₂HPO₄ at a pH of 7.4. The bacteria were cultured at 37°C in a rotation shaker for 18 hrs and harvested by centrifugation at 6,000 rpm for 20 minutes. The cells were washed twice using 0.1 M Phosphate buffer saline (PBS) solution with pH 7.4. Different cell concentrations were made, and their optical density (OD) was measured using UV-visible spectrophotometer at wavelength of 600 nm (OD_{600 nm}). The relationship between *E. coli* cell concentrations and OD_{600nm} values was established. The concentration of viable cells were estimated in terms of number of cells/mL using the spectrophotometric method at OD_{600 nm} (OD_{600nm} of 1.0 = 8 x 10⁸ cells/mL). The cell suspensions obtained were immediately used for subsequent electrochemical experiments. All the sample cultures were prepared on the day of the tests.

3.2.2 Optimization of parameters for bacteria-nanoparticles interaction studies

Electrochemical redox activity of *E. coli* / Ag-Au NPs complex was evaluated on glassy carbon electrode (Area = 0.071 cm²) using nano-impact electrochemistry. The electrochemical collision parameters such as applied potential, AC amplitude, supporting electrolyte concentration, nanoparticle volume, NPs molar ratio and NPs concentrations were optimized. UV-visible absorption changes as a result of interaction time, concentration (NPs and bacteria) were also investigated.

3.2.3 Sensors analytical parameters

The optimum interaction conditions were used to assess the potential of cyclic voltammetry, differential pulse voltammetry and EIS techniques for bacteria interaction using the synthesised Ag-Au (1:2) NPs. The μ Stat-i 400s potentiostat (Metrohm, Spain) instrument with a conventional three-electrode system was used to perform the entire electrochemical experiments. GCE with a diameter of 3 mm, Ag/AgCl (3.0 M KCl) and platinum wire (Pt) were used as working reference and counter electrodes respectively. Impedance measurements were performed in the frequency range of 0.1 Hz to 100 kHz at applied potential of 0.1 V and AC amplitude of 10 mV. All the experiments were performed at room temperature (25°C) and EIS results were fitted and modelled using Drop-view 8400 software interfaced with the potentiostat.

In all the experiments, alumina powder on micro-polish and polishing pads was used for cleaning the GC electrode. The electrode was sonicated for 10 minutes in ethanol/water (1:1 volumes) followed by air-drying before use. The GCE was finally activated by sweeping it to high anodic potential from + 0.6 to +1.3 V in 0.5 M H₂SO₄ versus Ag/AgCl, reference electrode, thoroughly rinsed using doubly distilled water and dried under a stream of nitrogen gas for 5 minutes. This was done to enhance the oxidation of the NPs hence facilitating their adsorption capacity onto the bacterial cell membranes for successful complex formation.

3.3 RESULTS AND DISCUSSION

3.3.1 Interaction of nanoparticles with bacteria

The interaction of the bacteria with the nanoparticles (Ag, Au and 2:1 Ag-Au) was assessed by monitoring the optical changes of the nanoparticles when they interact with the bacteria. Parameters that had an effect in these changes were determined. The effects of varying concentration of the *E. coli*, reaction time as well as the concentration of the nanomaterials were investigated. Figure 3-1 shows the UV-visible spectra changes observed with concentration increases of both *E. coli* and *Salmonella typhimurium* with NPs. From all the NPs studied, the optical changes noted were concentration, time and NPs type dependent. The absorbance increased with an increase in bacteria.

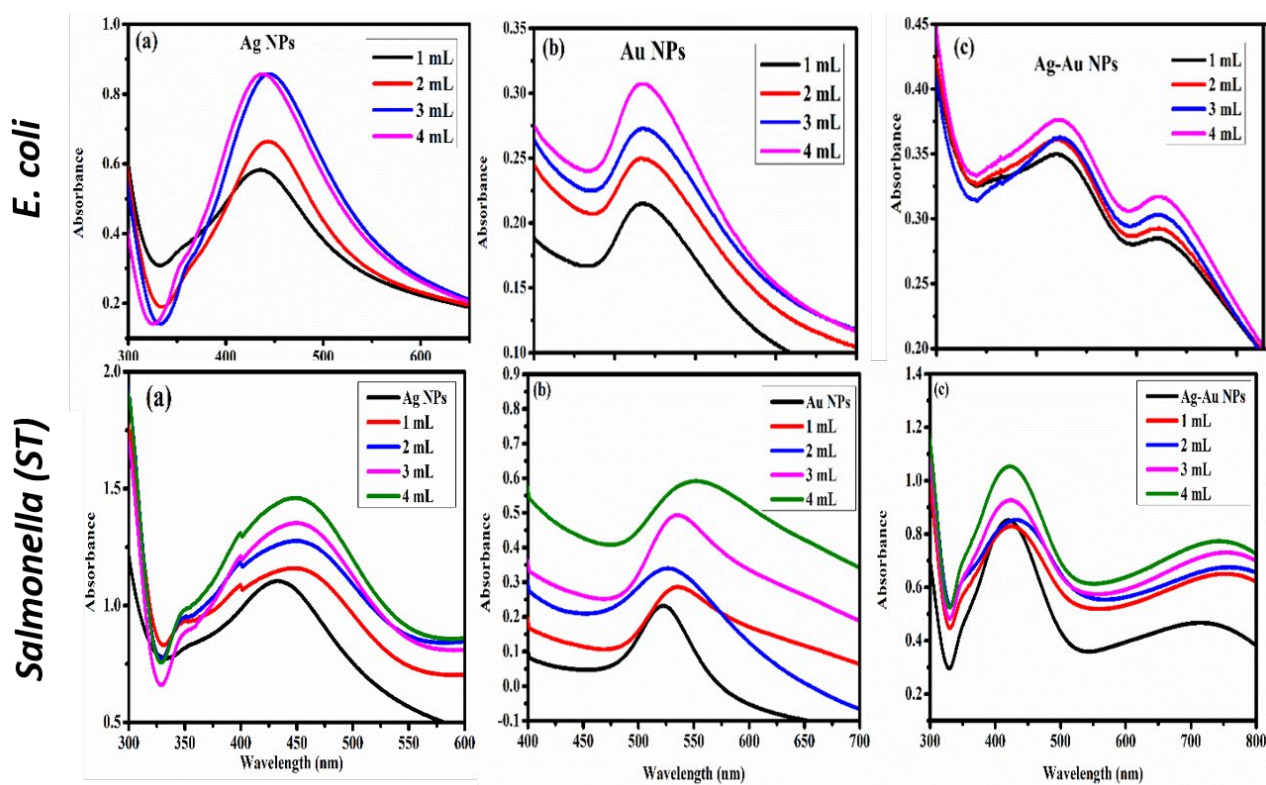


Figure 3-1: UV-visible absorption spectra interactions of various concentration of *E. coli* and *Salmonella typhimurium* bacteria with nanoparticles and (a) Ag NPs, (b) Au NPs and (c) Ag-Au (2:1) NPs

However, the changes in absorbance in both bacteria were more pronounced in Au Figure 3-1b compared to the Ag (Fig. 3-1a and the bimetallic Figure 3-1c) while a decrease in absorption was observed with time. Hence, a 20-minute interaction time was chosen as the appropriate time for analysis thus ensuring acceptable analysis time. Cyclic voltammogram of the NPs in absence and presence of the bacteria were recorded and depicted in Figure 3.2. From Figure 3-2 it is evident that the presence of the bacteria resulted to an observation of new peaks which are not observed in their absence. Hence, indicating a possibility of using electrochemistry techniques in detecting the bacteria. Both *E. coli* and *Salmonella typhimurium* have distinct peaks which have potential difference above 200 mV each. This potential difference indicates a possibility of carrying out simultaneous analysis of the bacteria.

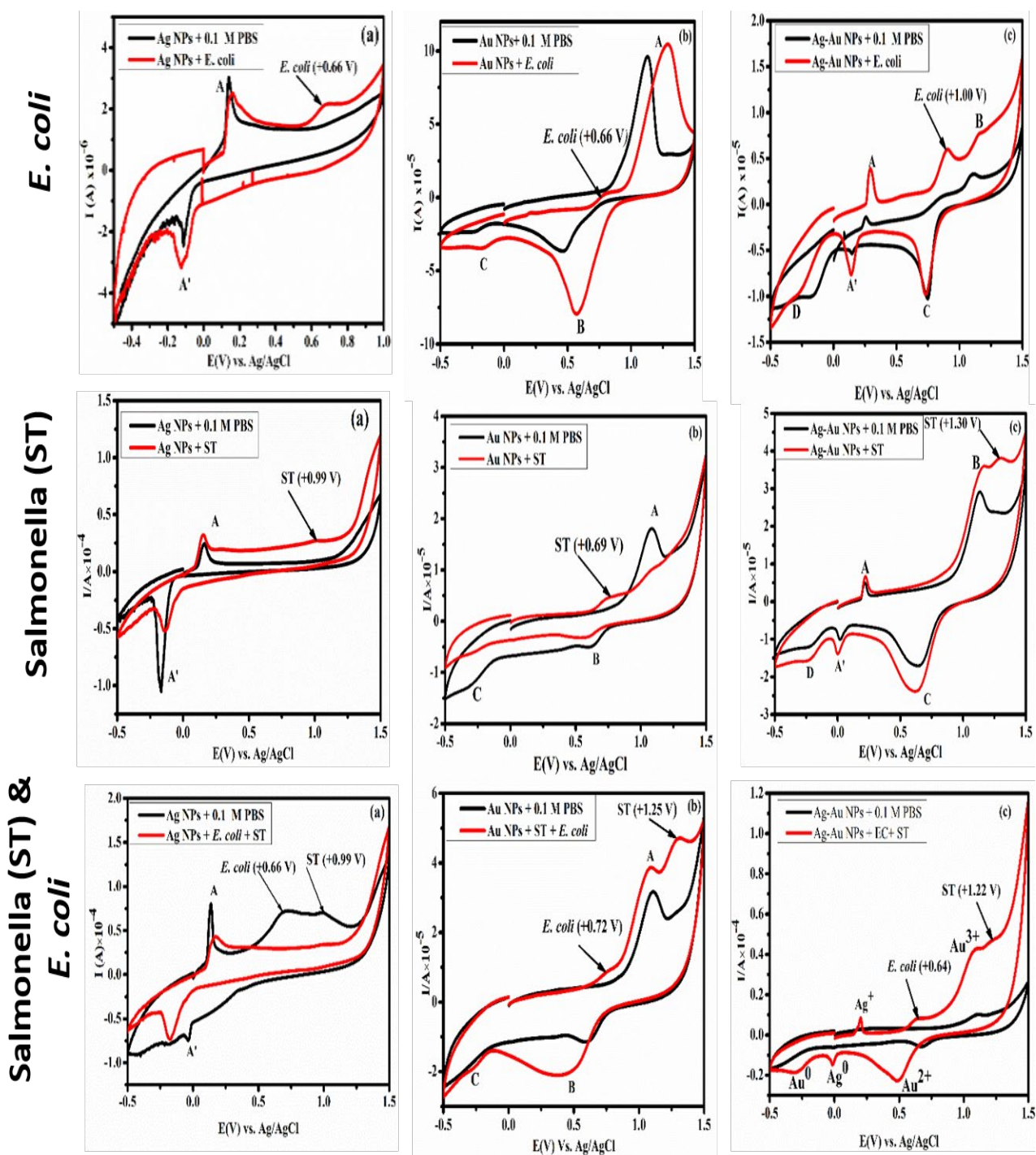


Figure 3-2: Cyclic voltammety detection of the *E. coli* and *Salmonella typhimurium* (ST) bacteria using a) Ag NPs, b) Au NPs and c) Ag-Au NPs in 0.1 M PBS. PH 7.4.

3.3.2 Sensor fabrication for detection of *E. coli*

The non-film sensors were chosen for the project in order to minimise sample analysis time by avoiding the minimum 3 hours that is usually required to ensure stable film. The detection of *E. coli* using the different electrochemistry techniques was assessed as in shown in Figure 3-3a and b. The possibility of detection was studied by DPV measuring the current in the absence and presence of the bacteria as shown in Figure 3-3.

The voltammograms for both *E. coli* and *Salmonella typhimurium* (ST) showed observable changes in the presence of monometallics and bimetallic NPs. In both cases the bimetallic showed higher current hence it was the NPs of choice for the sensors fabrication.

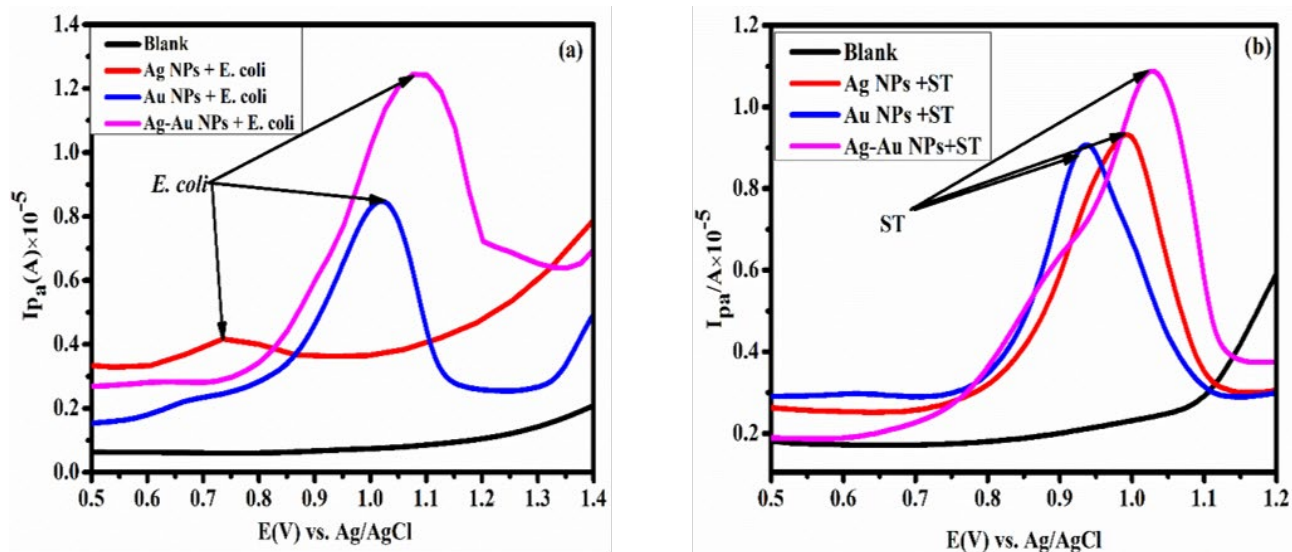


Figure 3-3: The differential pulse voltammograms (DPV) for detection of *E. coli* (a) and *Salmonella typhimurium* (b)

3.3.3 Sensor Optimisation

In order to obtain a reliable, accurate reproducible results the sensor fabrication and the transduction methodology were optimised. Optimisation was done by varying one parameter at a time while keeping all other parameters constants. Optimisation data for *E. coli* is depicted in Figure 3-4. Optimisation was two-fold; fabrication optimisation and method optimisation. Optimum conditions were chosen based on well-shaped, high current voltammograms with minimum background as well as the current signal. Figure 3-4 indicates graphs of current signals when varying method or fabrication parameters. The highest current observed in Figure 3-4 together with peak shapes were used to decide on optimum condition to use in further studies. The optimum conditions were used in calibration and validation analysis. The optimum conditions were found to be as follows:

EIS: interaction time 20 minutes; 5nM Ag-Au NPs; applied potential and AC amplitude of 0.1 V and 10 mV respectively at 0.050 V/s scan rate

DPV: Therefore, starting potential, modulation amplitude and modulation time of 0.5 V, 0.05 V and 0.025 s, respectively versus Ag/AgCl, reference electrode were chosen for further electrochemical studies at a scan rate of 0.03 V/s

Similar observations were found with *Salmonella typhimurium* and the data is not shown.

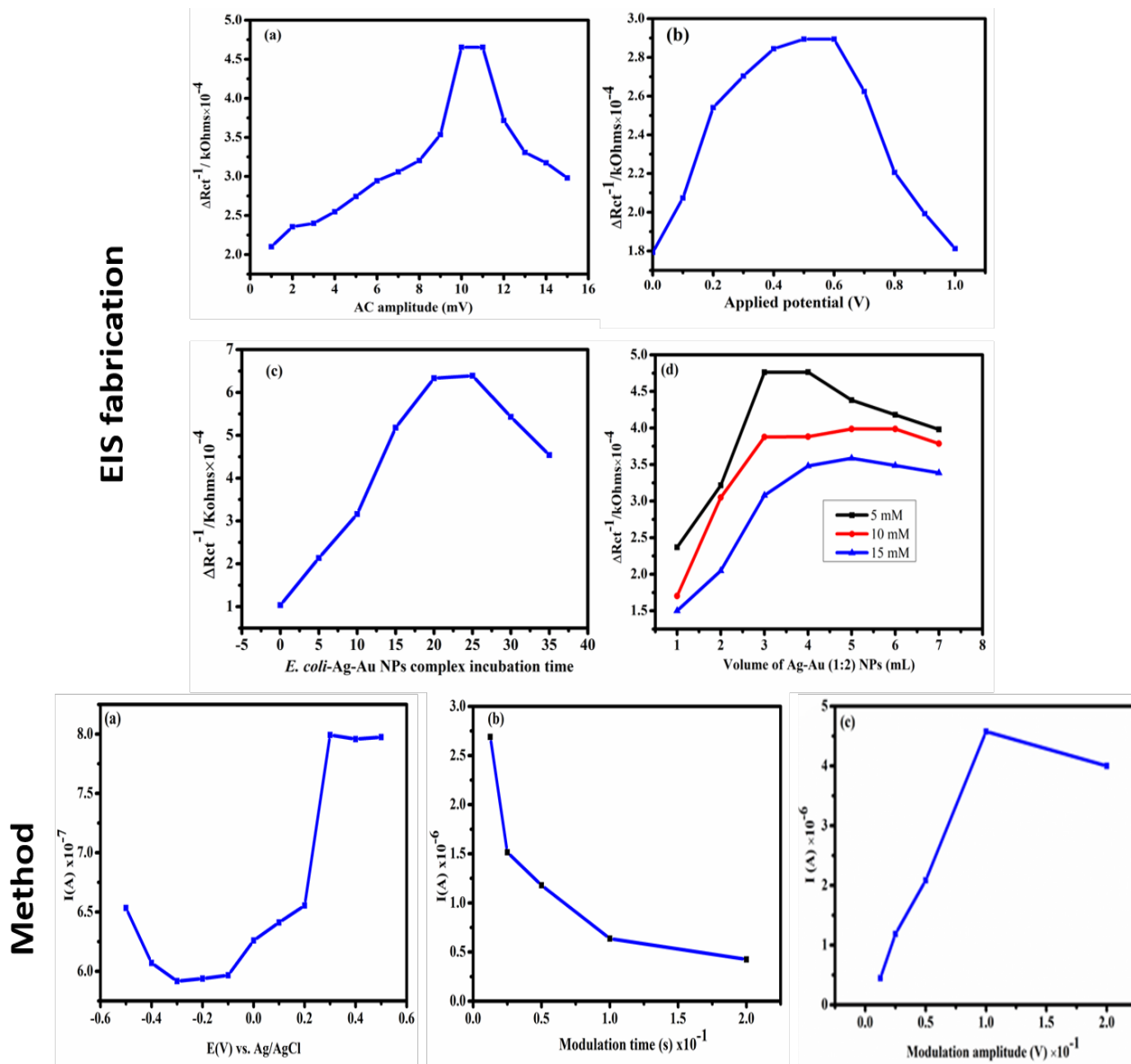


Figure 3-4: Sensor fabrication optimisation and experimental optimisation for DPV sensors

3.3.4 Calibration and analytical parameters

Analytical parameters were obtained using the optimum conditions. Various bacteria standards were measured using the three techniques (Fig. 3-5 and Fig. 3-6). The concentration signal plots (calibration graph) were linear. They were used to determine analytical parameters such as linear range and LOD.

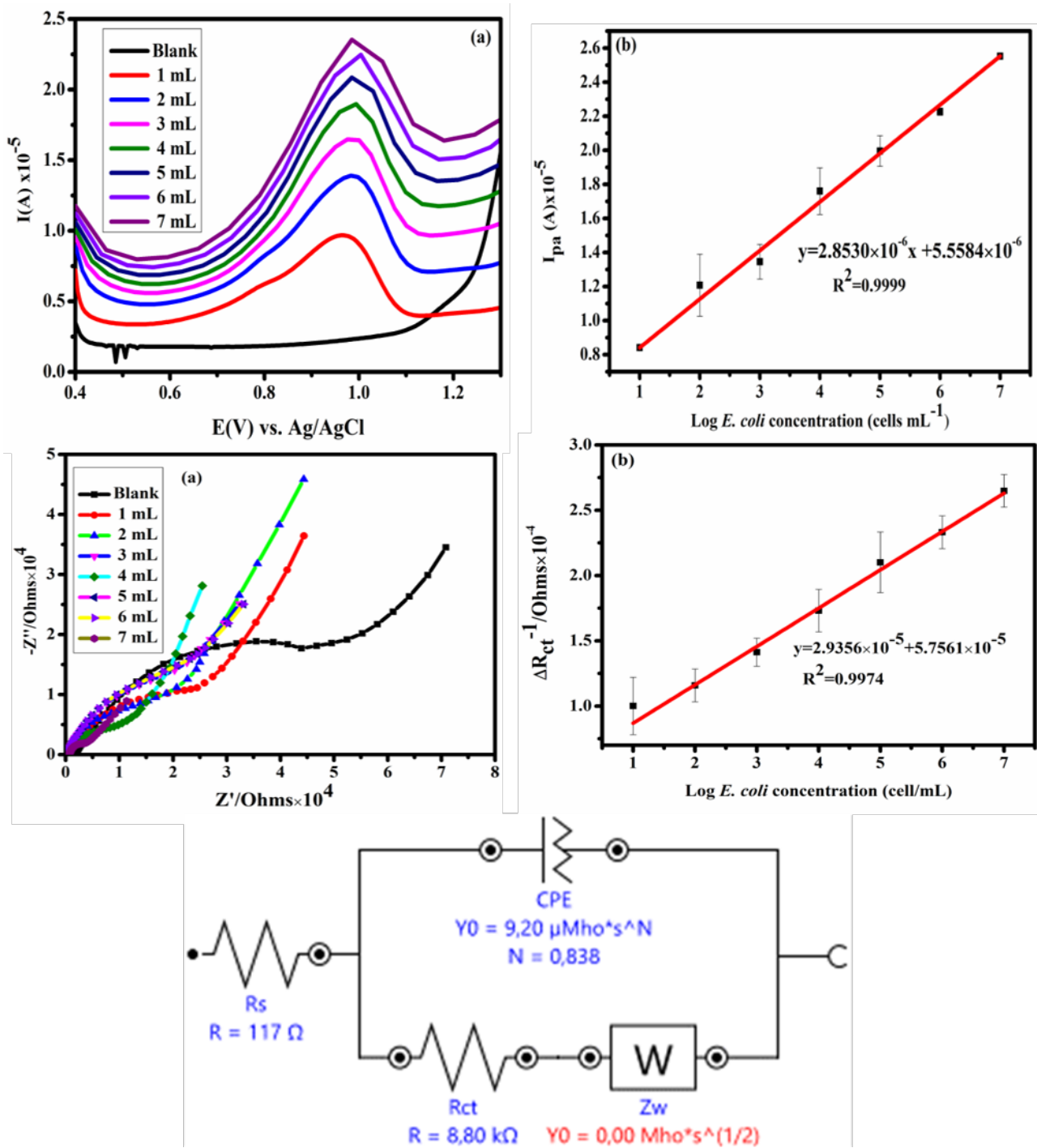


Figure 3-5 : Typical (a) DPV voltammograms and (b) EIS Nyquist plot responses of the sensors to varying concentrations of *E. coli* as well as the corresponding calibration plot of ΔR_{ct}^{-1} versus log of *E. coli* concentrations.

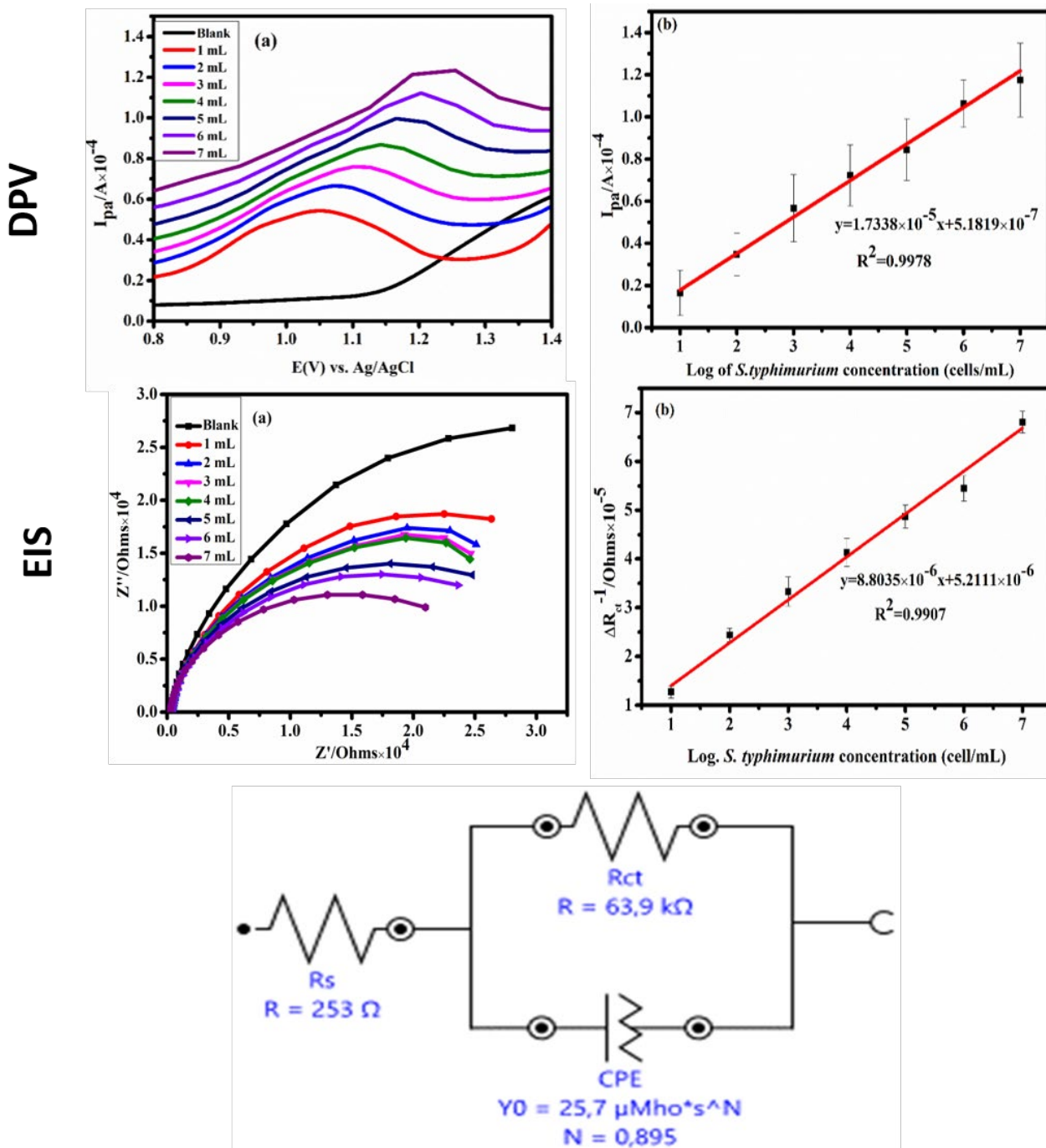


Figure 3-6: Typical (a) DPV voltammograms and (b) EIS Nyquist plot responses of the sensors to varying concentrations of *Salmonella typhimurium* as well as the corresponding calibration plot of ΔR_{ct}^{-1} versus log of *Salmonella typhimurium* concentrations.

The sensor was validated using recovery methods in spiked tap water (TW) and fruit juice (FJ). The spiked samples ΔR_{ct} were measured directly using EIS under optimized conditions. It was observed that the recovery studies of our method were in the range of (122.12±0.1 – 161.86±0.12) % FJ and (98.79±0.14-124.25± 0.15) % TW with significantly lower % RSD of (1.8-2.4) and (2.5-3.5) % for FJ and TW, respectively.

3.3.5 Mechanism for bacteria redox activity

The electrochemical transductions are based on monitoring of the redox activity of the bacteria. Electrons therefore move from the bacterial surface to the NPs which in turn became reduced. This interaction took place in the bulk supporting electrolyte. The resultant complex formed interacts with the active electrode surface, where the NPs became re-oxidized thus generating electrical signals at applied electrical potential. The more the NPs re-oxidized, the greater the redox activity hence rapid signal in differential pulse voltammetry (DPV), EIS and CV. The first two techniques were chosen based on their known low detection limits. EIS is also preferred due to its potential for use on site. The possible mechanism involved in each bacterium is suggested in Figure 3-7. The mechanisms identify the enzymes involved with each bacterium.

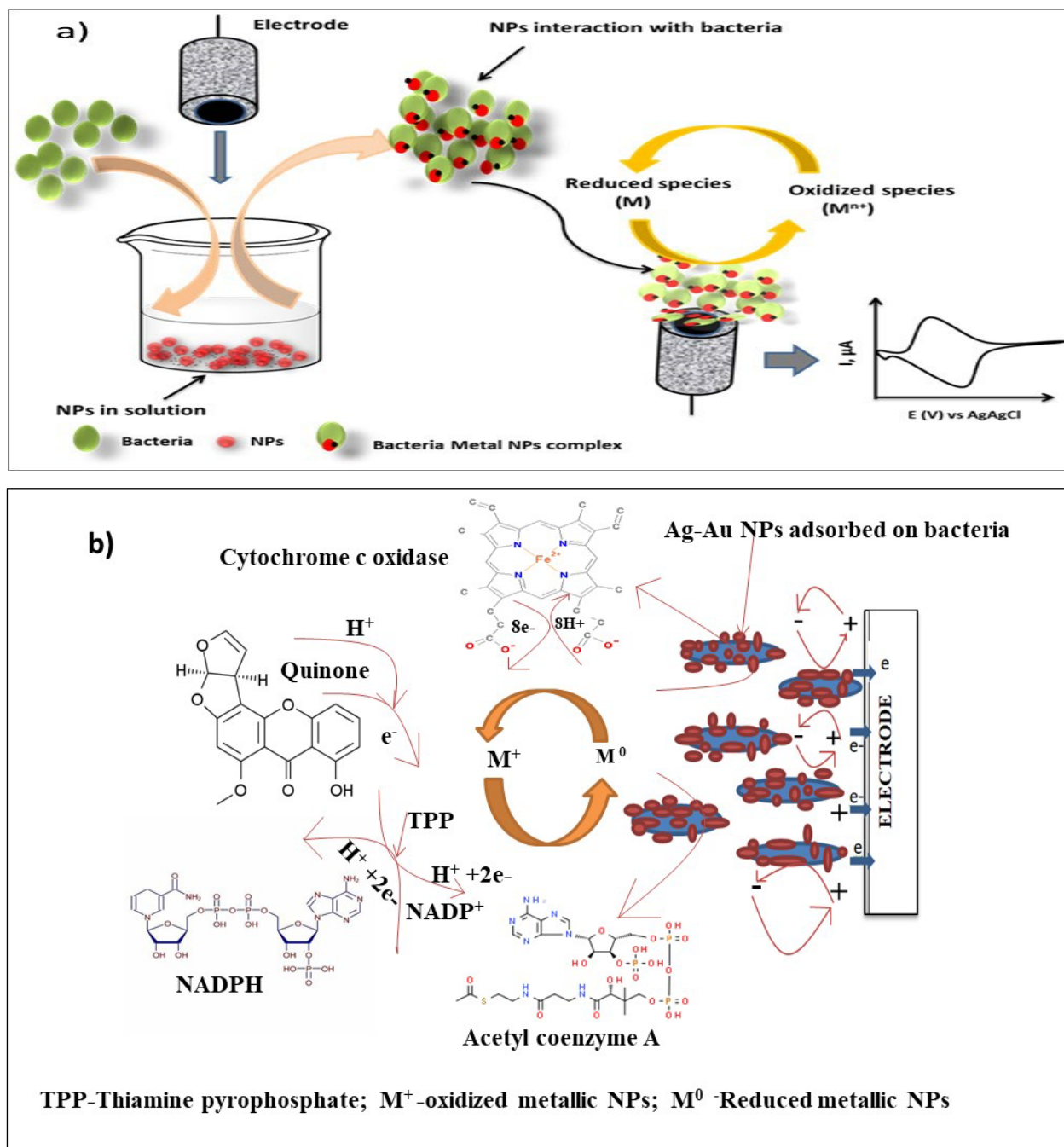


Figure 3-7: Mechanism of single bacterial redox activity analysis a) *Salmonella typhimurium* and b) *E. coli*.

The analytical parameters obtained were compared to literature values (Table 3-1). From the table few reports were made on LOD and LOQ and the dominating technique was amperometry (CA). Thus indicating a need to increase research in electrochemical transducer sensors in order to use them as alternatives to the microbiological plate techniques which are still dominating despite their laborious nature and 7 to 8 days' response. The sensors analytical parameters are analytically acceptable. Good standard deviations, LOD and LOQ as well as reasonable recoveries. These sensors developed can be used in water quality monitoring since their ranges are within the standard acceptable limits.

Table 3-1: Comparison of reported electrochemical techniques for *E. coli*^a and *Salmonella typhimurium*^b detection with the developed methods

Electrochemical technique	Detection platform	Electrolyte used	LOD (cells/mL)	LOQ (cells/mL)	Linear range (cells/mL)	Reference
DPV ^a	GCE (NIE) Ag-Au NPs	0.1 M PBS	2.3×10^1	3.1×10^3	10^1-10^7	This work
EIS ^a			1.8×10^1	2.3×10^2	10^1-10^8	
DPV ^b			2.5×10^1	4.0×10^1	10^1-10^7	
EIS ^b			1.2×10^1	4.0×10^2	10^1-10^9	
CA	Carbon-UME	0.1 M KCl	-	-	-	Chen et al., 2021
CA	Pt UME	0.1 M, Fe(CN) ₆ ⁴⁻	-	-	-	Guanye et al., 2018
CA	Pt-UME	0.001M, KCl	8.4×10^5	-	10^5-10^6	Ronspees and Thorgaard , 2018
CA	Au-UME	0.000869 M, TMPD-BF ₄	-	-	-	Couto , Chen , Kuss and Compton, 2018
CA	UME	0.02 M K ₄ Fe(CN) ₆	-	-	-	Lee et al., 2016
CA	Ag NPs-UME	0.1 M KCl	-	-	10^5-10^9	Sepunaru et al., 2015

3.4 SUMMARY

Sensors for detection and quantification of *E. coli* and *Salmonella typhimurium* were fabricated, optimised and analytical parameters determined through calibration graphs. The types of sensors developed were nano impact electrochemical sensors using glassy carbon electrode (GCE) assisted with bimetallic Ag-Au NPs. The electroanalytical techniques investigated were differential pulse voltammetry (DPV) and electrochemical impedance spectroscopy (EIS). All sensors had good analytical parameters as indicated by LOD, LOQ and linear ranges of 10^1 , 10^2 and 10^1-10^9 respectively. These values were comparable to the limited data found in the literature and can be applicable in environmental monitoring as they incorporate the WHO recommended limits.

CHAPTER 4: CONCLUSION AND RECOMMENDATIONS

4.1 CONCLUSIONS

- The chemical synthesis and characterisation of nanomaterials (CuO, ZnO, Ag, Au and Ag-Au NPs) and AgInS core QDs and AgInS/ZnS core/shell were successfully done. Both spectroscopic and electrochemical characterisation confirmed the synthesis of the targeted materials.
- The NPs bacteria interaction investigations were carried out using UV-visible absorption spectra and electrochemistry.
- The interactions were observed to be concentration, time and type of NPs dependent. The worst interactions were observed with quantum dots while bimetallic Ag-Au NPs showed more interaction with the bacteria hence it was further utilised in the development of the sensors. Further studies of quantum dots are recommended because they have a fast reaction time which made it difficult to observe changes resulting to concentration changes. A fast reaction time is important in reducing analysis time.
- Three different electrochemical techniques sensors (cyclic voltammetry, differential pulse voltammetry and EIS) were fabricated, optimised and calibration graphs obtained for determination of analytical parameters and sensor sensitivity. The sensors were optimised and validated using recovery studies in real sample mediums of Juice and tap water. Real sample testing of the sensors is recommended as well as validation using an approved method.
- The developed sensors analytical parameters were comparable to reported data in the literature. Presently, literature lack a lot of the necessary information for electrochemical bacteria detection.
- From the three electrochemical sensors studied both DPV and EIS transduction showed higher sensitivity and lower detection limits. Only reproducibility was tested. Therefore, the stability of the sensors as well as the ability to reuse is recommended.
- The sensors have very low detection limits, thus indicating a high possibility of their application in environmental analysis which is predominantly based on trace analysis. Therefore, these sensors are ideal for monitoring *E. coli* and *Salmonella typhimurium* contamination in water and food. The analysis is fast with minimum sample preparation. However, sample preparation for food sample will require optimisation to ensure accuracy.
- A recommendation of these sensors in surface water analysis both in laboratory and at the point of sampling is recommended. This would require municipality permit; hence it was not achieved within the timeframe. However, the permit is still being pursued.

4.2 RECOMMENDATIONS

- Further work on interdigitated electrodes to study the possibility of simultaneous detection of *Salmonella typhimurium* and *E. coli* will still continue once the digitated nanoarrays electrodes were only supplied in January. The nanoarrays purchase was a problem due to import controls during lockdown and restricted movement.
- Further quantum dots studies are recommended because they showed a fast interaction rate resulting in very little observable changes in optical properties. A different technique can be used that is more sensitive and the quantum dots concentration can be modulated.
- In order to ensure the commercial usage of these sensors the NPs stability has to be assessed. The stability studies are important especially for onsite analysis.
- They have to be a comparable study of onsite and offsite using different electrochemical techniques.

REFERENCES

1. Cabral, J.P., *Water microbiology. Bacterial pathogens and water*. International Journal of Environmental Research and Public Health, 2010. **7**(10): p. 3657-3703.
2. Allocati, N., Masuilli, M., Alexeyev and Di Ilio C.; *Escherichia coli in Europe: an overview*. International Journal of Environmental Research and Public Health, 2013. **10**(12): p. 6235-6254.
3. Nicolas-Chanoine, M.-H., X. Bertrand and J.-Y. Madec, *Escherichia coli ST131, an intriguing clonal group*. Clinical Microbiology Reviews, 2014. **27**(3): p. 543-574.
4. Ferens, W.A. and C.J. Hovde, *Escherichia coli O157: H7: animal reservoir and sources of human infection*. Foodborne Pathogens And Disease, 2011. **8**(4): p. 465-487.
5. Heredia, N. and S. García, *Animals as sources of food-borne pathogens: A review*. Animal nutrition, 2018. **4**(3): p. 250-252.
6. Todd, E.C.D, Greig J D, Bartleson CA and Michaels BS., *Outbreaks where food workers have been implicated in the spread of foodborne disease. Part 4. Infective doses and pathogen carriage*. Journal of Food Protection, 2008. **71**(11): p. 2339-2373.
7. Ansari, S., Sherchand JB, Parajuli K, Mishra SK, Dahal RK, Sherestha S, Tandukar S and Pokhrel BM., *Bacterial etiology of acute diarrhea in children under five years of age*. Journal of Nepal Health Research Council, 2013.
8. WHO. Progress in drinking water, sanitation and Hygiene 2017 update and SDG baselines: world health organisation (WHO); United Nations Children's Fund (UNICEF; Geneva, Switzerland 2017.
9. Li, Y., Cheng P, Gong J, Fang L, Deng J, Liang W and Zheng J., *Amperometric immunosensor for the detection of Escherichia coli O157: H7 in food specimens*. Analytical Biochemistry, 2012. **421**(1): p. 227-233.
10. Stromberg, Z.R., Johnson JR, Fairbrother JM, Kilbourne J, Van Goor A, Rd RC and Mellata M., *Evaluation of Escherichia coli isolates from healthy chickens to determine their potential risk to poultry and human health*. PloS one, 2017. **12**(7): p. e0180599.
11. Freedman, S.B., Xie J, Neufeld MJ, Hamilton WL, Hartling L and Tarr PI., *Shiga toxin-producing Escherichia coli infection, antibiotics, and risk of developing hemolytic uremic syndrome: a meta-analysis*. Clinical Infectious Diseases, 2016. **62**(10): p. 1251-1258.
12. Schiller, L.R., D.S. Pardi and J.H. Sellin, *Chronic diarrhea: diagnosis and management*. Clinical Gastroenterology and Hepatology, 2017. **15**(2): p. 182-193. e3.
13. Plaza, N.,Castello D, Perz-Reytor D, Higuera G, Garcia K and Bastias R., *Bacteriophages in the control of pathogenic vibrios*. Electronic Journal of Biotechnology, 2018. **31**: p. 24-33.25.
14. Hilton, S.K., Castro-Nallar E, Perz-Losada M, Toma I , McCaffrey TA, Hoffman EP, Siegel MO , Simon GL, Johnson QE and Crandall KA., *Metataxonomic and metagenomic approaches vs. culture-based techniques for clinical pathology*. Frontiers in microbiology, 2016. **7**: p. 484.
15. Zhang, X-Y, Li Z-Y, Zhaang Y, Zang X-Q, Ueno K, Misawa H and Sn K, *Bacterial Concentration Detection using a PCB-based Contactless Conductivity Sensor*. Micromachines, 2019. **10**(1): p. 55.
16. Smith, S, Mager D, Perebikovskiy A, Shamloo E, Kinahan D, Mishra R, Delgado SMT, Kido H, Saha S, Ducree J, Madou M, Land K and Korvink JG, *CD-based microfluidics for primary care in extreme point-of-care settings*. Micromachines, 2016. **7**(2): p. 22.

17. Walper, SA, Argones GL, Sapsford KE, Brown III CW, Rowland CE, Breger JC and Merdintz IL, *Detecting biothreat agents: From current diagnostics to developing sensor technologies*. ACS sensors, 2018. **3**(10): p. 1894-2024.
18. Niessen, L, Luo J, Denschlag C and Vogel RF, *The application of loop-mediated isothermal amplification (LAMP) in food testing for bacterial pathogens and fungal contaminants*. Food Microbiology, 2013. **36**(2): p. 191-206.
19. Umesha, S. and H. Manukumar, *Advanced molecular diagnostic techniques for detection of food-borne pathogens: Current applications and future challenges*. Critical Reviews in Food Science And Nutrition, 2018. **58**(1): p. 84-104.
20. Wang, Y, Z. Ye and Y. Ying, *New trends in impedimetric biosensors for the detection of foodborne pathogenic bacteria*. Sensors, 2012. **12**(3): p. 3449-3471.
21. Arora, S., Ahamed N, Sucheta and Siddiui S, *Detecting food borne pathogens using electrochemical biosensors: An overview*. IJCS, 2018. **6**(1): p. 1031-1039.
22. Ojea-Jiménez, I., N.G. Bastús and V. Puentes, *Influence of the sequence of the reagents addition in the citrate-mediated synthesis of gold nanoparticles*. The Journal of Physical Chemistry C, 2011. **115**(32): p. 15752-15757.
23. Rafique Muhammad, Uhammad Shahid Rafique, Shariqa hassn butt, umber kalsoom, Amina Afzal, SAFia Anjum and Arslan USmanet; *Dependence of the structural optical and thermo-physical properties of gold nano-particles synthesized by laser ablation method on the nature of laser*. Optik, 2017. **134**: p. 140-141.
24. Chen, Yafei, Denchao wang, Yanran Liu, Guanyue Gao and Jinfaang Zhi; *Redox activity of single bacteria revealed by electrochemical collision technique*. Biosensors and Bioelectronics, 2021. **176**: p. 112914.
25. Gao Guanye, Dengchao wang, Ricardo Brocenschi, Jinfang Zhi and Michael v Mirkin; *Toward the detection and identification of single bacteria by electrochemical collision technique*. Analytical Chemistry, 2018. **90**(20): p. 12123-12130.
26. Lee Ji Young, Byung-Know Kim, Mijoeng Kang and Jung Hui Park; *Label-free detection of single living bacteria via electrochemical collision event*. Scientific Reports, 2016. **6**(1): p. 1-6.
27. Sepunaru Lior, Kristina Tschulik, Christopher Batchelor-McAuley, Rachel Gavish and Richard G. Compton. *Electrochemical detection of single E. coli bacteria labelled with silver nanoparticles*. Biomaterials Science, 2015. **3**(6): p. 816-820.
28. Ronspees, A.T. and S.N. Thorgaard, *blocking electrochemical collisions of single E. coli and B. subtilis bacteria at ultramicroelectrodes elucidated using simultaneous fluorescence microscopy*. Electrochimica Acta, 2018. **278**: p. 412-420.
29. Rosa A.s Couto, Lifu Chen, Sabina Kuss and Richard G Compton, *Detection of Escherichia coli bacteria by impact electrochemistry*. Analyst, 2018. **143**(20): p. 4840-4843.
30. Gunda N.S.K., Dasgupta S., Mitra S.K., *DipTest: A litmus test for E. coli detection in water*. Plos one <https://doi.org/10.1371/journal.pone.0183234>, 2017, P1